Desalination and Water Treatment
www.deswater.com

doi: 10.5004/dwt.2022.28586

264 (2022) 196–204
July

Simulation of chromium(III) ions biosorption from aqueous environment by olive stone biomass in a fixed-bed column and analysis of effective parameters using computational fluid dynamics method

Amir Hossein Saeedi Dehaghani[a,*], Reza Soleimani[b], Amir H. Mohammadi[c,*]

[a]*Department of Petroleum Engineering, Faculty of Chemical Engineering, Tarbiat Modares University, Tehran, Iran, email: asaeedi@modares.ac.ir*
[b]*Department of Chemical Engineering, Faculty of Chemical Engineering, Tarbiat Modares University, Tehran, Iran, email: soleimanire@gmail.com*
[c]*Discipline of Chemical Engineering, School of Engineering, University of KwaZulu-Natal, Howard College Campus, King George V Avenue, Durban 4041, South Africa, email: amir_h_mohammadi@yahoo.com*

Received 14 December 2021; Accepted 22 May 2022

ABSTRACT

In this study, Langmuir and dose-response models for chromium(III) ion biosorption from aqueous environment in a fixed-bed system are presented. Conservation and momentum equations for adsorption of metals ions are solved using computational fluid dynamics method with COMSOL multiphysics software. Simulation results for dose-response model show good agreement with experimental data. Also, a parametric study was conducted to investigate the effects of porosity, bed height, the input flow rate and the concentration of chromium(III) ion. Moreover, individual systems, two-component and three-component chromium, copper, lead and cadmium ions are studied. The results show that cadmium ion has the lowest, and copper ion has the highest penetration curve breakdown.

Keywords: Heavy metal ion; Chromium(III); Biosorption; Fixed-bed; Computational fluid dynamics; Aqueous solution

1. Introduction

Heavy metals ions in water are one of the most serious environmental problems in recent years, which are elements with atomic masses between 63.5 and 200.6 g/gmol and specific gravities more than 5 g/cm^3 [1]. With the rapid development of industries such as mining, the fertilizer industry, the battery industry, the paper industry and so on, a huge amount of such pollutants enters the environment through wastewater [2–4]. Unlike organic compounds, heavy metals ions are not biodegradable and, over time, accumulate in the bodies of humans and animals, which cause many diseases in humans [5]. Serious diseases such as various cancers have researchers taking suitable methods to remove heavy metals ions from wastewater [6] so that, in addition to the adsorption of these metal ions, it is economical and the environment is not affected adversely in the aftermath. As a result, the separation of heavy metals ions from wastewater and contaminated groundwater is essential. Various traditional technologies are used to remove cations from water, such as filtration, ion exchange, reverse osmosis, and membrane filters. Due to the overuse of chemicals, the use of these methods yields high cost, and they cannot be used in small-scale and household level [7]. These traditional methods also suffer from other disadvantages like incomplete toxic heavy metals ions removal, high reagent and energy supply and the production of toxic sludge.

* Corresponding authors.

Biosorption, which is an adsorptive process and involves the use of different biomass or natural substances, has recently received more attention as an attractive alternative for up-taking heavy metals ions from wastewater as it offers several advantages over traditional techniques such as, eco-friendly nature, excellent performance and low cost [8,9].

A literature survey reveals that for the last decade, biosorption has been widely investigated for the removal of different heavy metals ions from aqueous solutions [9–26].

The majority of biosorption studies reported in the literature have been carried out in batch reactors and generally, adsorption data obtained in such systems can't address the practical challenges associated with most treatment systems [27]. Indeed, for a large scale of treatment, biosorption processes are performed continuously, mostly in fixed-bed columns [8]. However, the literature review reveals that publications about biosorption of heavy metals ions in fixed-bed column mode are scarce [28,29]. From the process modeling viewpoint, the breakthrough curve (the effluent concentration-time profile) is used to describe the dynamic behavior of a fixed-bed column [30]. The removal effectiveness of the column, the adsorption capacity of the adsorbent and the position and shape of breakthrough curves are dependent variables influenced by operational conditions such as inlet concentration, feed flow rate and feed flow rate along with the bed depth and inlet diameter factors [31]. Very important and useful information can be extracted from the dynamic equilibrium analyses in columns like the system size, contact time and adsorbent usage rate, which can be attained from breakthrough curves [32,33]. Thus, it is evident that the modeling of the concentration time profile is highly needed in successful design and reliable operation of an industrial fixed-bed column for the biosorption process [12].

In this direction, recently, a number of research has applied various simple mathematical models for modeling and describing the biosorption of heavy metals ions in fixed-bed. Lim and Aris [34] found an increase of flow rate and initial concentration cause to reduce the saturation of the column. They also showed that Thomas model has a better agreement with adsorption of cadmium ion data in comparison with Yoon–Nelson and Adam Buharet models. Chowdhury et al. [35] showed good agreement between continuous systems and the Langmuir isotherm results. The Redlich–Kovich isotherm way was found to be chemically adsorbed. In column studies, BDST and Thompson models showed good agreement. Izquierdo et al. [36] reported that the results of discontinuous system are in good agreement with Langmuir isotherm for the maximum capacity sorbent of 85.78 mg/g. They also studied different concentrations of continuous systems and showed the maximum capacity of 56.7 mg/g in the column. Lodeiro et al. [37] applied the BDST model to simulate the adsorption process in a fixed-bed, and also Adam Buhart-Yan and Beltran and Chu models were considered to study the match with experimental data. Their results demonstrated Yan model had a better agreement. Borba et al. [38] applied multi-component differential equations to evaluate the hydrodynamic and adsorption process of nickel ions removal from aqueous environment by Saragvsam biosorption in the fixed-bed. Aksu and Gönen [39] showed good agreements of Langmuir and Freundlich isotherms and experimental data of phenol adsorption by the activated sludge in a fixed-bed. Silva et al. [40] showed that Langmuir isotherm has a better agreement in comparison of Freundlich isotherm in discontinuous system for adsorption of copper ions by the Saragasvm adsorbent. In the same approach, Han et al. [41] studied the effects of column height, flow rate, the concentration of methylene blue in the input stream applying Thomas model to find the optimal operating condition. The effects of different heights on the bed on thrust curves were also obtained using BDST model.

Computational fluid dynamics (CFD) is a simulation tool that uses numerical analysis and data structures to model fluid flow situations. The main advantage of CFD method is its high ability to solve efficiently different physical domains simultaneously, also in a coupled way [42]. Since CFD technique can be of great help to environmental engineering and processing, over the last few years or so, application of CFD method in such areas has been increased [43,44].

Generally, several modes of transport and processes such as permeation, convection, diffusion, mass transport, fluid flow and physical and chemical adsorption occur simultaneously in a continuous fixed-bed column during biosorption of heavy metals ions [42] and the aim of CFD method is to empower the academic community and engineers to model effectively the channel-fluidic phenomena in such adsorption processes [42,45,46].

The literature review of CFD method in modeling such areas shows that in 2015, Oliver et al. [47] used CFD simulations to observe mixing inside the electrochemical reactors for Cr(VI) ion reduction from wastewater. They observed that the array for the rotating ring electrodes with 4 vertical fins operating at 130 rpm has the highest flow/power ratio, and the lowest mixing time. Martínez-Delgadillo et al. [48] examined the impacts of kinds of electrochemical reactor inlet on performance by means of CFD simulation. Their results show that the electrochemical reactor gives the best performance whilst it operates with the Tangential inlet. In another study, by conducting experiments along with applying a CFD model, the performance of an electrochemical reactor with the ring electrodes rotating was assessed at different speeds at which the electrochemical process was utilized in order to eliminate Cr(VI) ion from wastewater [49]. Recently, Karpinska and Bridgeman [43] provided a complete review on CFD modelling of activated sludge systems.

Considering the critical role of removing heavy metals ions, to the authors' knowledge, there is a lack of computational modeling tools to investigate the heavy cations biosorption mainly in continuous fixed-beds system. In this paper, a CFD model with COMSOL multiphysics software is expressed for uptake of heavy metals ions viz. chromium, copper, lead and cadmium ions. Applying the literature experimental data of chromium ion (III) biosorption in a fixed-bed system with olive stone [8], the adsorption models were evaluated and, using an appropriate model, a multi-component system adsorption was studied. Also, the important design parameters such as effects of porosity, bed height, the input flow rate and the concentration of chromium on the breakthrough curves were investigated.

2. Governing equations

Based on the recent modeling approaches, researchers have applied the equations and a variety of conditions, as well as traditional, modern, and some smart conditions for modeling processes. The purpose of numerical methods is to study the heavy metals ions adsorption models inside the fixed-bed system and evaluate the effects of operational parameters in order to achieve the most optimized design which takes a lot of time and high costs in laboratory. Herein, the transport phenomena modeling for the fixed-bed is solved using CFD technique with COMSOL software (Version 4.4) based on the Finite Element Method (FEM), for sorption systems including one-, two- and multi-metal mixtures of cations. It includes a coupled system of partial differential, ordinary differential and algebraic equations illustrating the dynamics of the multicomponent ion exchange in a flow-through fixed-bed.

2.1. Model geometry

The geometry of the model in this work is as two symmetrical dimensions. To do this, a rectangle with a width of 1.5 cm and height of 23 cm was drawn.

2.2. Equations and definition of physical models

In the fixed-bed system, a small element with Δz height is selected as the volume control. It is assumed that the flow is one dimension and is cross-sectional along the bed. The balance of adsorbent material in the bed uses partial differential equations for the solute in the liquid phase inlet and adsorbed in solid phase $z\to 0$ [42,50]:

$$\frac{\partial C_{\mathrm{bi}}}{\partial t}=-u\frac{\partial C_{\mathrm{bi}}}{\partial z}+D_L\frac{\partial^2 C_{\mathrm{bi}}}{\partial z^2}-\frac{\left(1-\varepsilon_p\right)}{\varepsilon_p}\rho_p\frac{\partial q_i}{\partial t} \tag{1}$$

For video capture influence ($\partial q_i/\partial t$), these data is as follows [42,50]:

$$\frac{\partial q_i}{\partial t}=\frac{3k_{\mathrm{fi}}}{R_p\rho_p}\left(C_{\mathrm{bi}}-C_{\mathrm{pi},R=R_p}\right) \tag{2}$$

Substituting ($\partial q_i/\partial t$) from Eq. (2) into Eq. (1) yields:

$$-D_L\frac{\partial^2 C_{\mathrm{bi}}}{\partial z^2}+u\frac{\partial C_{\mathrm{bi}}}{\partial z}+\frac{\partial C_{\mathrm{bi}}}{\partial t}+\frac{3k_{\mathrm{fi}}\left(1-\varepsilon_p\right)}{\rho_p R_p}\left[C_{\mathrm{bi}}-C_{\mathrm{pi},R=R_p}\right]=0 \tag{3}$$

Equation of continuity within the pores of the particles can be stated as follows:

$$\varepsilon_p\frac{\partial C_{\mathrm{pi}}}{\partial t}+\left(1-\varepsilon_p\right)\rho_p\frac{\partial q_i}{\partial t}-\varepsilon_p D_{\mathrm{pi}}\left[\frac{1}{R_p^2}\frac{\partial}{\partial R}\left(R^2\frac{\partial C_{\mathrm{pi}}}{\partial R}\right)\right]=0 \tag{4}$$

The initial and boundary conditions include:

$$t=0: C_{\mathrm{bi}}=C_{\mathrm{bi}}\left(0,z\right)=0; C_{\mathrm{pi}}=C_{\mathrm{pi}}\left(0,R,z\right)=0 \tag{5}$$

$$Z=0:\frac{\partial C_{\mathrm{bi}}}{\partial z}=\frac{u}{D_L}\left(C_{\mathrm{bi}}-C_{\mathrm{oi}}\right); Z=L:\frac{\partial C_{\mathrm{bi}}}{\partial z}=0 \tag{6}$$

$$R=0:\frac{\partial C_{\mathrm{pi}}}{\partial R}=0; R=R_p:\frac{\partial C_{\mathrm{pi}}}{\partial R}=\frac{k_{\mathrm{fi}}}{\varepsilon_p D_{\mathrm{pi}}}\left[C_{\mathrm{bi}}-C_{\mathrm{pi},R=R_p}\right] \tag{7}$$

Langmuir isotherm equation and dose-response for a number of components are as follows [42,50]:

$$q_i=\frac{q_{\mathrm{mi}}b_i C_{\mathrm{oi}}c_{\mathrm{pi}}}{1+\sum_{j=1}^{N}b_j C_{\mathrm{oi}}c_{\mathrm{pj}}}\quad\text{Langmuir} \tag{8}$$

$$\frac{C}{C_i}=1-\frac{1}{1+\left(\frac{C_i V_{\mathrm{ef}}}{q_0 m}\right)^a}\qquad\text{Dose}-\text{Response} \tag{9}$$

Substituting Eq. (8) into Eqs. (3) and (4) yield semi-dimensionless Eqs. (10) and (11), respectively, as follows:

$$-D_L\frac{\partial^2 c_{\mathrm{bi}}}{\partial z^2}+u\frac{\partial c_{\mathrm{bi}}}{\partial z}+\frac{\partial c_{\mathrm{bi}}}{\partial t}+\frac{3k_{\mathrm{fi}}\left(1-\varepsilon_p\right)}{\rho_p R_p}\left[c_{\mathrm{bi}}-c_{\mathrm{pi},R=R_p}\right]=0 \tag{10}$$

$$\left[\varepsilon_p+\left(1-\varepsilon_p\right)\rho_p\frac{\partial q_i}{C_{\mathrm{pi}}}\right]\frac{\partial c_{\mathrm{pi}}}{\partial t}=\frac{\varepsilon_p D_{\mathrm{pi}}}{R_p^2}\frac{\partial^2 c_{\mathrm{pi}}}{\partial r^2}+\frac{2\varepsilon_p D_{\mathrm{pi}}}{R_p^2 r}\frac{\partial c_{\mathrm{pi}}}{\partial r}=0 \tag{11}$$

As a result, initial and boundary conditions are as follows:

$$t=0: c_{\mathrm{bi}}=c_{\mathrm{bi}}\left(0,z\right)=0; c_{\mathrm{pi}}=c_{\mathrm{pi}}\left(0,R,z\right)=0 \tag{12}$$

$$z=0:\frac{\partial c_{\mathrm{bi}}}{\partial z}=\frac{u}{D_L}\left(c_{\mathrm{bi}}-C_{\mathrm{oi}}\right); z=L:\frac{\partial c_{\mathrm{bi}}}{\partial z}=0 \tag{13}$$

$$r=0:\frac{\partial c_{\mathrm{pi}}}{\partial r}=0; r=1:\frac{\partial c_{\mathrm{pi}}}{\partial r}=\frac{R_p k_{\mathrm{fi}}}{\varepsilon_p D_{\mathrm{pi}}}\left[c_{\mathrm{bi}}-c_{\mathrm{pi},R=R_p}\right] \tag{14}$$

The simulated parameters are provided in Table 1.

Finite element method discretizes the domain of governing equations, and a big linear equation system is generated, which can be shown as:

$$\mathrm{FP}=S \tag{15}$$

Matrixes F and S are known here, and matrix P is unknown. One approach to calculate this matrix is the calculation of F^{-1}, but it will not be cost effective, because it will have lots of non-zero components and besides many calculations, a huge memory is needed to store them. The method of matrix decomposition to L and U members (upper and lower triangular matrixes), or in other words using direct

solvers, is used to overcome this problem. In this topic, researchers have presented various algorithms such as MUMPS, UMFPACK, LU, PARDISO and SuiteSparseQR which all do try to create *U* and *L* members with the least non-zero components. Herein, PARDISO technique was applied in order to solve equations, and matrix *F* was divided into two matrixes named *L* and *U* through graph theory. The coefficients matrix has the minimum of non-zero components during the decomposition, with the purpose of the faster calculations as well as low memory. In the calculations, the numerical solver of Parallel Sparse Direct Solver (PARDISO) version 5.0.0 was used as linear solver. A PC with 2.67 GHz Intel®Core (TM) i5 CPU M 480 and RAM 4.00 GB (2.98 GB usable) 64-bit operating system was used for running. The triangular mesh elements within the volume were utilized and arrayed to give satisfactory resolution for boundary layers nearby the fluid-solid interfaces. Various numerical tests were executed at different mesh resolutions to eliminate enhancement in mesh size and quality of modeling results.

Table 1
Dose-response model parameters for four investigated concentration levels

Parameter	C_i (ppm)			
	10	25	50	75
a	1.561	1.065	0.719	1.135
b	395.3	168.7	70.87	54.16
q_o (mg/g)	0.263	0.281	0.236	0.271

3. Results and discussion

In this study, the experimental data [8] match with the dose-response and Langmuir models have been reviewed. The results show that the model can well simulate the adsorption of the chromium(III) ions in the ground filled with olive ash. Fig. 1 shows the correspondent to the experimental data at concentrations of 10, 25, 50 and 75 mg/L with chromium(III) Langmuir adsorption and dose-response models.

The effects of the concentration parameters, porosity and adsorption of chromium(III) ions in the input fixed column with olive core ash were investigated. To evaluate the initial concentration effect on the column performance, different values (10, 25, 50 and 75 ppm) were used, while other terms were fixed. Breaches Chart shows that initial increase of concentration will increase slope. Slope increase is due to that by increasing the initial concentration, mass transfer driving force increases. Also, increasing the driving force causes the increase in the initial concentration in the pores of the adsorbent which can also increase the adsorption

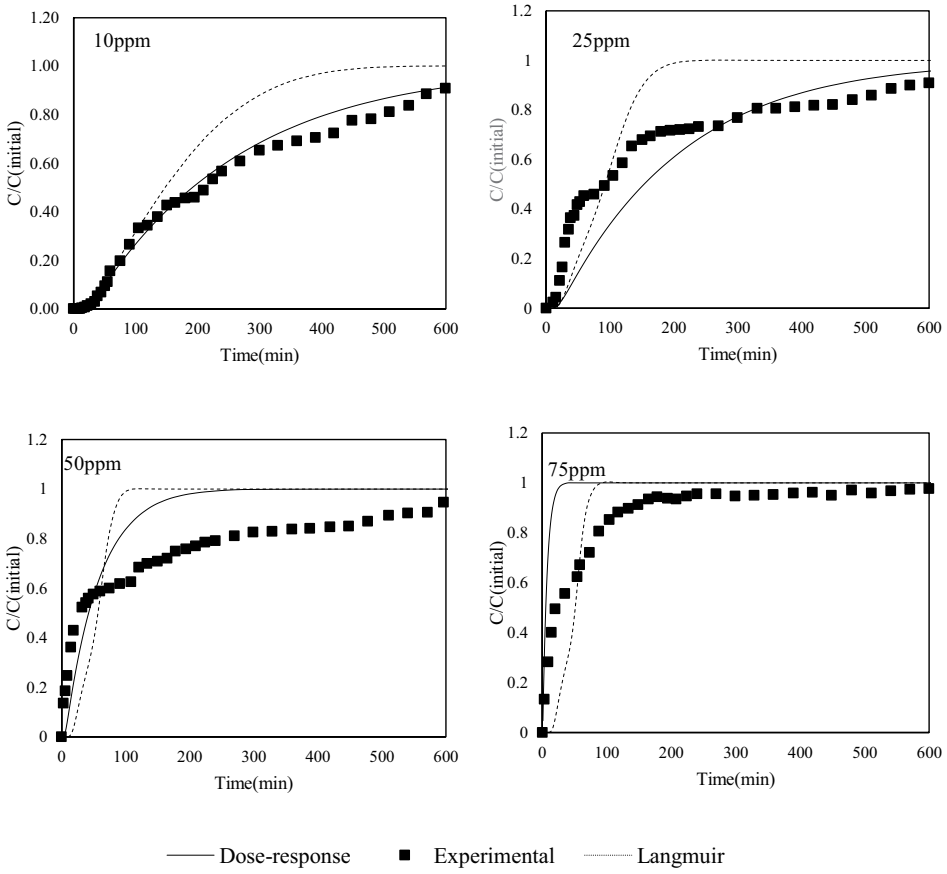

Fig. 1. Comparison of experimental data [8] fit with Langmuir adsorption and dose-response models at different concentrations.

rate to be equalized. In other words, quickly reaching saturation increases with reduction in the initial concentration. Also, this chart can be verbal that the penetration rate is controlled by the concentration gradient (Fig. 2).

With constant circumstances, the effect of porosity was investigated. Fig. 3 shows that with the increase in porosity, reaching to the point of failure increases, because by reducing the particle size, porosity reduces and the surface areas of the particles increase. Therefore, by increasing the surface area, the more adsorption sites for the adsorption of solute molecules occur which increases the adsorption time in adsorbed filling sites. Thus increasing the particle size increases, the thickness of the surface layer around the particles to be settled which increases the time of the particles to reach the surface of adsorbent.

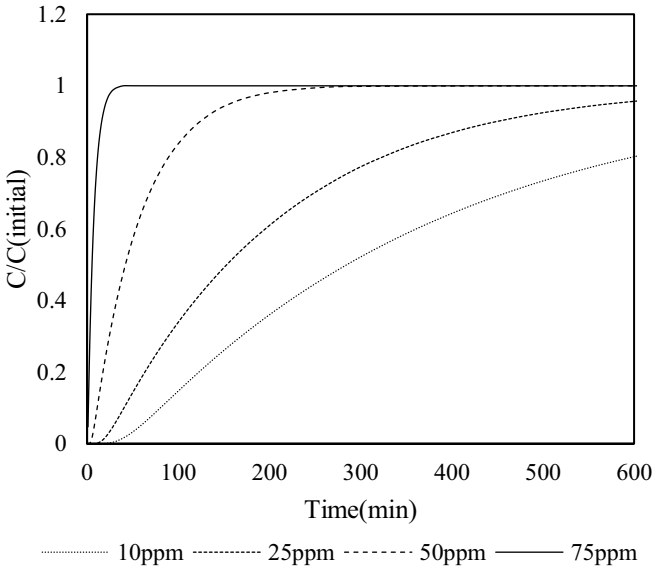

Fig. 2. Effect of initial concentration on the adsorption chromium.

The effects of the inlet flow rate (2, 6 and 12 mL/min) are given in Fig. 4. As can be seen in this figure, by increasing the flow rate of inputs, slope of breaches also increases. The failure point reduces with an increase in rate curves, which is due to reduced pollution retention time in the column in a way that the time to balance in high flow rate is too low. As a result, at high flow rates, the contact time between adsorbent and adsorbate decreases. In addition, at high flow rates, the rate of mass transfer increases, which leads to quicker saturation.

Finally, the systems with a few minor metals were studied. Metals ions adsorption for copper, lead, cadmium and chromium ions, independently, are reviewed in two-components and multi-components. Input flow rate, initial concentration, porosity and temperature, respectively were selected as 2×10^{-6} m^3/min, 0.1923 mol/m^3, 0.335, 25°C, respectively. Fig. 5 shows the adsorption of these metals ions independently.

Figs 6 and 7, respectively, show two-component and three-component adsorption systems. As the charts from the simulation of adsorption process fueled by olive core ash shows, cadmium ions are the strongest and copper ions are the weakest adsorbed, because copper ions have the highest failed time and cadmium ions have the least failure time in the breakthrough curve. After cadmium ions, chromium ions, lead ions, and copper ions, respectively, have less time to failure in breakthrough curve which can be seen in two-part and three-part systems. The results of the simulation in a single component system also complies with the results of multi-component systems and results are expressed almost the same.

Active adsorption sites form the core ash of olives. These active sites proposed to strong and weak adsorbents will be filled by adsorbents. In competition between strong and weak adsorption capacities, strong adsorbent immediately enter into operation and start filling active sites. But weakened adsorb the active sites later and weaker. Because of this in the multi-component systems, it is observed that

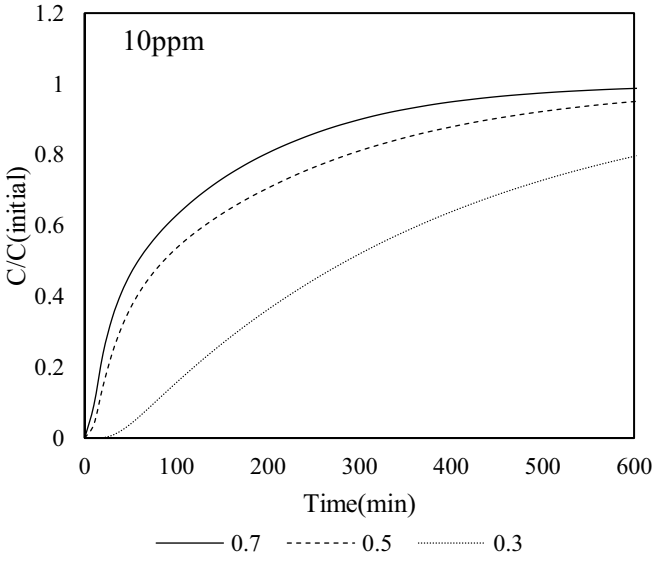

Fig. 3. Effect of porosity on the adsorption of chromium ions.

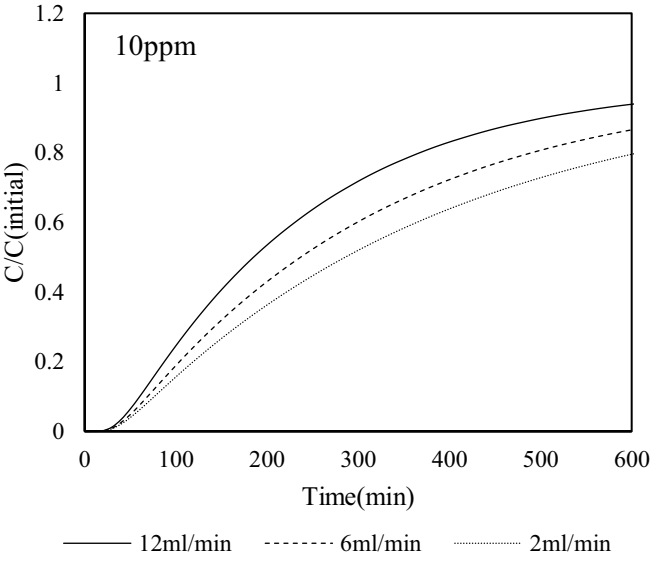

Fig. 4. Effect of input flow rate on adsorption of chromium ions.

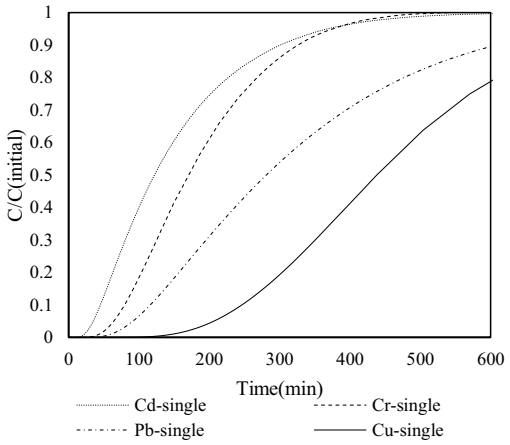

Fig. 5. Graph of heavy metals ions in the fixed-bed independently.

copper or lead ions do not even reach their initial concentrations in the output, because their metal ion rivals are strong adsorbents and saturated active sites sooner.

4. Conclusion

In the current study, chromium(III) ions biosorption by olive stone in a continues fixed-bed column was simulated using CFD method. According to the discussions on the simulation results, the following conclusions and recommendation can be drawn:

- Effect of porosity (range between 0.3 and 0.7), the input flow rate (range between 2 to 12 mL/min) and the initial concentration of chromium (range between 10 to 75 ppm) was investigated. The results show that lowering the initial concentration and lowering input flow rate as well as porosity within the studied ranges, is desirable.

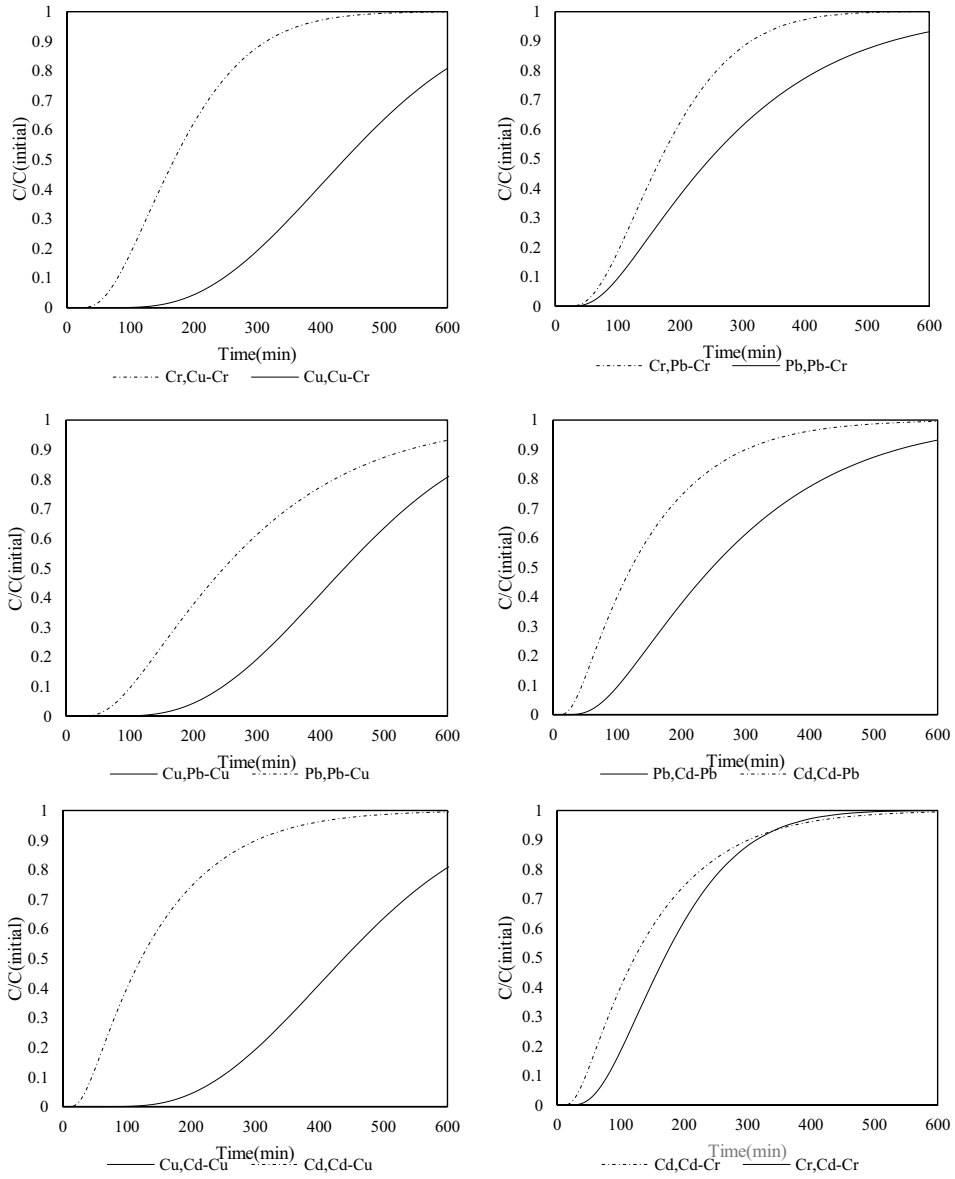

Fig. 6. The two-component heavy metals ions adsorption systems by the fixed-bed.

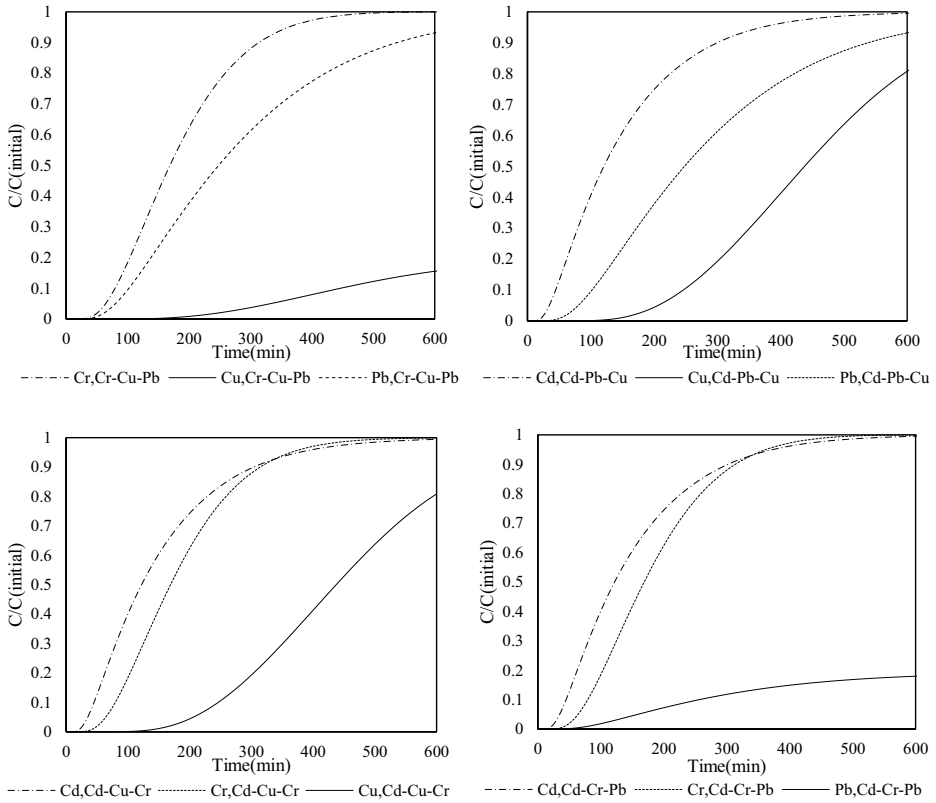

Fig. 7. The three-component heavy metals adsorption systems by the fixed-bed.

- Multi-components biosorption process including cadmium, chromium, lead, and copper biosorption was analyzed. The results show that cadmium ions are quickly adsorbed and after that, chromium ions, lead ions, and copper ions, respectively, have less time to failure in breakthrough curve, that is, they are more likely adsorbed in the active sites, correspondingly.
- The simulation results by dose response model show that there is a high consistency and well agreement with the experimental ones, which indicates that to address challenges with conducting experiments in the laboratory such as being time consuming and high costs, the applied computational model, viz. CFD, can be used as an effective tool in biosorption processes for analyzing different parameters.

Symbols and abbreviations

a	—	Constant
b_i	—	Langmuir constant, min^{-1}
C_{bi}	—	Concentration of solute i in the fluid phase of the column, kg/m^3
c_{bi}	—	Scaled concentration of solute i in the fluid phase of the column C_{bi}/C_{oi}
C_{oi}	—	Initial concentration of solute i, mg/L
C_{pi}	—	Concentration of solute i in the fluid phase within the pores, kg/m^3
c_{pi}	—	Scaled concentration of solute i in the fluid phase within the pores C_{pi}/C_{oi}
D_{pi}	—	Pore diffusion coefficient of component i, m^2/s
D_L	—	Axial dispersion coefficient, m^2/s
k_{fi}	—	External mass transfer coefficient of solute i, m/s
L	—	Bed height, m
m	—	Mass of sorbent, g
q_o	—	Maximum concentration of the solute in the solid phase, mg/g
q_{mi}	—	Adsorption equilibrium constant defined by Langmuir equation of component i, mg/g
R_p	—	Radius of particle, m
R	—	Radial distance in the particle, m
R_p	—	Radius of particle, m
r	—	Scaled radial distance in the particle R/R_p
t	—	Time, s
u	—	Velocity, m/s
V_{ef}	—	Volume of the effluent, mL

Greek

ε_p	—	Particle porosity
ρ_p	—	Density of particle, kg/m^3

Subscripts

j	—	Integer value
p	—	Pore phase

References

[1] B.W. Atkinson, F. Bux, H.C. Kasan, Considerations for application of biosorption technology to remediate metal-contaminated industrial effluents, Water SA, 24 (1998) 129–135.
[2] C. Brierley, J. Brierley, Immobilization of biomass for industrial application of biosorption, Biohydrometallurgical Technol., 2 (1993) 35–44.
[3] G. Naja, C. Mustin, B. Volesky, J. Berthelin, A high-resolution titrator: a new approach to studying binding sites of microbial biosorbents, Water Res., 39 (2005) 579–588.
[4] M.C. Palmieri, B. Volesky, O. Garcia Jr., Biosorption of lanthanum using *Sargassum fluitans* in batch system, Hydrometallurgy, 67 (2002) 31–36.
[5] Z. Aksu, Application of biosorption for the removal of organic pollutants: a review, Process Biochem., 40 (2005) 997–1026.
[6] S.P.K. Sternberg, R.W. Dorn, Cadmium removal using *Cladophora* in batch, semi-batch and flow reactors, Bioresour. Technol., 81 (2002) 249–255.
[7] Z. Zulfadhly, M.D. Mashitah, S. Bhatia, Heavy metals removal in fixed-bed column by the macro fungus *Pycnoporus sanguineus*, Environ. Pollut., 112 (2001) 463–470.
[8] M. Calero, F. Hernáinz, G. Blázquez, G. Tenorio, M.A. Martín-Lara, Study of Cr(III) biosorption in a fixed-bed column, J. Hazard. Mater., 171 (2009) 886–893.
[9] A. Chatterjee, S. Schiewer, Biosorption of cadmium(II) ions by citrus peels in a packed bed column: effect of process parameters and comparison of different breakthrough curve models, CLEAN–Soil, Air, Water, 39 (2011) 874–881.
[10] C. Bertagnolli, M.G.C. da Silva, E. Guibal, Chromium biosorption using the residue of alginate extraction from *Sargassum filipendula*, Chem. Eng. J., 237 (2014) 362–371.
[11] J. Plaza Cazón, C. Bernardelli, M. Viera, E. Donati, E. Guibal, Zinc and cadmium biosorption by untreated and calcium-treated *Macrocystis pyrifera* in a batch system, Bioresour. Technol., 116 (2012) 195–203.
[12] A.B. Pérez Marín, M.I. Aguilar, J.F. Ortuño, V.F. Meseguer, J. Sáez, M. Lloréns, Biosorption of Zn(II) by orange waste in batch and packed-bed systems, J. Chem. Technol. Biotechnol., 85 (2010) 1310–1318.
[13] A.G. Tekerlekopoulou, M. Tsiflikiotou, L. Akritidou, A. Viennas, G. Tsiamis, S. Pavlou, K. Bourtzis, D.V. Vayenas, Modelling of biological Cr(VI) removal in draw-fill reactors using microorganisms in suspended and attached growth systems, Water Res., 47 (2013) 623–636.
[14] P.S. Vankar, R. Sarswat, A.K. Dwivedi, R.S. Sahu, An assessment and characterization for biosorption efficiency of natural dye waste, J. Cleaner Prod., 60 (2013) 65–70.
[15] J. Plaza Cazón, M. Viera, E. Donati, E. Guibal, Zinc and cadmium removal by biosorption on *Undaria pinnatifida* in batch and continuous processes, J. Environ. Manage., 129 (2013) 423–434.
[16] M.S. Seyed Dorraji, A.R. Amani-Ghadim, Y. Hanifehpour, S. Woo Joo, A. Figoli, M. Carraro, F. Tasselli, Performance of chitosan based nanocomposite hollow fibers in the removal of selenium(IV) from water, Chem. Eng. Res. Des., 117 (2017) 309–317.
[17] H.-L. Song, L. Liang, K.-Y. Yang, Removal of several metal ions from aqueous solution using powdered stem of *Arundo donax* L. as a new biosorbent, Chem. Eng. Res. Des., 92 (2014) 1915–1922.
[18] H. Cui, F. Li, B. Ren, C. Xue, C. Cui, J.-Y. Wang, Biosorption of aquatic Pb^{2+}, Hg^{2+}, and Cd^{2+} using a combined biosorbent—*Aspergillus niger*-treated rice straw, Sep. Sci. Technol., 53 (2018) 626–635.
[19] M.X. Loukidou, T.D. Karapantsios, A.I. Zouboulis, K.A. Matis, Cadmium(II) biosorption by *Aeromonas caviae*: kinetic modeling, Sep. Sci. Technol., 40 (2005) 1293–1311.
[20] B. Ramesh Naik, Ch. Suresh, N.V. Sandeep Kumar, K. Seshaiah, A.V.R. Reddy, Biosorption of Pb(II) and Ni(II) ions by chemically modified *Eclipta alba* stem powder: kinetics and equilibrium studies, Sep. Sci. Technol., 52 (2017) 1717–1732.
[21] K. Parvathi, R. Nagendran, Biosorption of chromium from effluent generated in chrome-electroplating unit using *Saccharomyces cerevisiae*, Sep. Sci. Technol., 42 (2007) 625–638.
[22] Y. Sağ, B. Akçael, T. Kutsal, Ternary biosorption equilibria of chromium(VI), copper(II), and cadmium(II) on *Rhizopus arrhizus*, Sep. Sci. Technol., 37 (2002) 279–309.
[23] Y. Sağ, A. Kaya, T. Kutsal, Biosorption of lead(II), nickel(II), and copper(II) on *Rhizopus arrhizus* from binary and ternary metal mixtures, Sep. Sci. Technol., 35 (2000) 2601–2617.
[24] A. Sarı, M. Tuzen, Biosorption of As(III) and As(V) from aqueous solution by lichen (*Xanthoria parietina*) biomass, Sep. Sci. Technol., 45 (2010) 463–471.
[25] R. Say, N. Yılmaz, A. Denizli, Biosorption of cadmium, lead, mercury, and arsenic ions by the fungus *Penicillium purpurogenum*, Sep. Sci. Technol., 38 (2003) 2039–2053.
[26] J. Shah, M.R. Jan, A. ul Haq, M. Sadia, Biosorption of cadmium from aqueous solution using mulberry wood sawdust: equilibrium and kinetic studies, Sep. Sci. Technol., 46 (2011) 1631–1637.
[27] M. Masomi, A.A. Ghoreyshi, H. Radnia, K. Pirzadeh, Adsorption of Fe(II) from aqueous phase by chitosan: application of physical models and artificial neural network for prediction of breakthrough, Int. J. Eng. Trans. B, 26 (2013) 845–858.
[28] M.C. de Hoces, G. Blázquez García, A.R. Gálvez, M.A. Martín-Lara, Effect of the acid treatment of olive stone on the biosorption of lead in a packed-bed column, Ind. Eng. Chem. Res., 49 (2010) 12587–12595.
[29] K. Vijayaraghavan, J. Jegan, K. Palanivelu, M. Velan, Biosorption of copper, cobalt and nickel by marine green alga *Ulva reticulata* in a packed column, Chemosphere, 60 (2005) 419–426.
[30] M.A. Martín-Lara, F. Hernáinz, G. Blázquez, G. Tenorio, M. Calero, Sorption of Cr(VI) onto olive stone in a packed bed column: prediction of kinetic parameters and breakthrough curves, J. Environ. Eng., 136 (2010) 1389–1397.
[31] A.R. Keshtkar, F. Kafshgari, M.A. Mousavian, Binary biosorption of uranium(VI) and nickel(II) from aqueous solution by Ca-pretreated *Cystoseira indica* in a fixed-bed column, J. Radioanal. Nucl. Chem., 292 (2012) 501–512.
[32] A.M.D. Canteli, D. Carpiné, A. de Paula Scheer, M.R. Mafra, L. Igarashi-Mafra, Fixed-bed column adsorption of the coffee aroma compound benzaldehyde from aqueous solution onto granular activated carbon from coconut husk, LWT Food Sci. Technol., 59 (2014) 1025–1032.
[33] C. Moreno-Castilla, Adsorption of organic molecules from aqueous solutions on carbon materials, Carbon, 42 (2004) 83–94.
[34] A.P. Lim, A.Z. Aris, Continuous fixed-bed column study and adsorption modeling: removal of cadmium(II) and lead(II) ions in aqueous solution by dead calcareous skeletons, Biochem. Eng. J., 87 (2014) 50–61.
[35] S. Chowdhury, S. Chakraborty, P.D. Saha, Response surface optimization of a dynamic dye adsorption process: a case study of crystal violet adsorption onto NaOH-modified rice husk, Environ. Sci. Pollut. Res., 20 (2013) 1698–1705.
[36] M. Izquierdo, C. Gabaldón, P. Marzal, F.J. Álvarez-Hornos, Modeling of copper fixed-bed biosorption from wastewater by *Posidonia oceanica*, Bioresour. Technol., 101 (2010) 510–517.
[37] P. Lodeiro, J. Barriada, R. Herrero, M.S. de Vicente, The marine macroalga *Cystoseira baccata* as biosorbent for cadmium(II) and lead(II) removal: kinetic and equilibrium studies, Environ. Pollut., 142 (2006) 264–273.
[38] C.E. Borba, R. Guirardello, E.A. Silva, M.T. Veit, C.R.G. Tavares, Removal of nickel(II) ions from aqueous solution by biosorption in a fixed-bed column: experimental and theoretical breakthrough curves, Biochem. Eng. J., 30 (2006) 184–191.
[39] Z. Aksu, F. Gönen, Biosorption of phenol by immobilized activated sludge in a continuous packed bed: prediction of breakthrough curves, Process Biochem., 39 (2004) 599–613.
[40] E.A. da Silva, E.S. Cossich, C.R.G. Tavares, L. Cardozo Filho, R. Guirardello, Modeling of copper(II) biosorption by marine alga *Sargassum* sp. in fixed-bed column, Process Biochem., 38 (2002) 791–799.
[41] R. Han, Y. Wang, W. Yu, W. Zou, J. Shi, H. Liu, Biosorption of methylene blue from aqueous solution by rice husk in a fixed-bed column, J. Hazard. Mater., 141 (2007) 713–718.
[42] H. Esfandian, A. Samadi-Maybodi, B. Khoshandam, M. Parvini, Experimental and CFD modeling of diazinon pesticide removal

using fixed-bed column with Cu-modified zeolite nanoparticle, J. Taiwan Inst. Chem. Eng., 75 (2017) 164–173.
[43] A.M. Karpinska, J. Bridgeman, CFD-aided modelling of activated sludge systems – a critical review, Water Res., 88 (2016) 861–879.
[44] A.N. Kochevsky, Possibilities of simulation of fluid flows using the modern CFD software tools, arXiv Preprint Physics/0409104, (2004) 1–12.
[45] T. Glatzel, C. Litterst, C. Cupelli, T. Lindemann, C. Moosmann, R. Niekrawietz, W. Streule, R. Zengerle, P. Koltay, Computational fluid dynamics (CFD) software tools for microfluidic applications – a case study, Comput. Fluids, 37 (2008) 218–235.
[46] W. Qian, J. Wu, L. Yang, X. Lin, Y. Chen, X. Chen, J. Xiong, J. Bai, H. Ying, Computational simulations of breakthrough curves in cAMP adsorption processes in ion-exchange bed under hydrodynamic flow, Chem. Eng. J., 197 (2012) 424–434.
[47] H.-C. Oliver, R.-A. Yonatan, V.X. Mendoza-Escamilla, M. Helvio, M.A. Morales-Mora, S.A. Martínez-Delgadillo, The effect of internal impellers on mixing in an electrochemical reactor with rotating rings electrodes, Chem. Eng. Process. Process Intensif., 88 (2015) 37–46.
[48] S.A. Martínez-Delgadillo, H.R. Mollinedo P., M.A. Gutiérrez, I.D. Barceló, J.M. Méndez, Performance of a tubular electrochemical reactor, operated with different inlets, to remove Cr(VI) from wastewater, Comput. Chem. Eng., 34 (2010) 491–499.
[49] S. Martinez-Delgadillo, H. Mollinedo-Ponce, V. Mendoza-Escamilla, C. Gutiérrez-Torres, J. Jiménez-Bernal, C. Barrera-Diaz, Performance evaluation of an electrochemical reactor used to reduce Cr(VI) from aqueous media applying CFD simulations, J. Cleaner Prod., 34 (2012) 120–124.
[50] A.H. Sulaymon, S.A. Yousif, M.M. Al-Faize, Competitive biosorption of lead mercury chromium and arsenic ions onto activated sludge in fixed-bed adsorber, J. Taiwan Inst. Chem. Eng., 45 (2014) 325–337.